Langmuir

Article

pubs.acs.org/Langmuir

Impact of Particulate Antigens, Such as *Bacillus anthracis*, on the Uniformity of Response across a Biosensor Flow Cell As Determined by GC-SPR

Nicola E. Cant* and Sarah E. Harrison

Detection Department, Dstl Porton Down, Salisbury, Wiltshire. SP4 0JQ, U.K.

ABSTRACT: Biosensors are desired for the detection of a wide range of analytes in various scenarios, for example environmental monitoring for biological threats, from toxins to viruses and bacteria. Ideally a single sensor will be capable of simultaneous multianalyte detection. The varying nature, and in particular disparate size, of such a variety of analytes poses a significant challenge in the development of effective high-confidence instruments. Many existing biosensors employ functionalized flow cells in which spatially defined arrays of surface-immobilized recognition elements, such as antibodies, specifically capture their analyte of interest. To function optimally, arrays should provide equivalent responses for equivalent events across their active area. Experimental data obtained using a grating coupled surface plasmon resonance (GC-SPR) instrument, the BIAcore Flexchip, have revealed differences in response behaviors between proteinaceous and particulate analytes. In particular, the magnitude of responses seen with *Bacillus anthracis* spores appears to be influenced by shear and gravitational effects while those from soluble proteins are more uniform. We have explored this dependence to understand its fundamental impact on the successful implementation of multianalyte environmental biological detection systems.

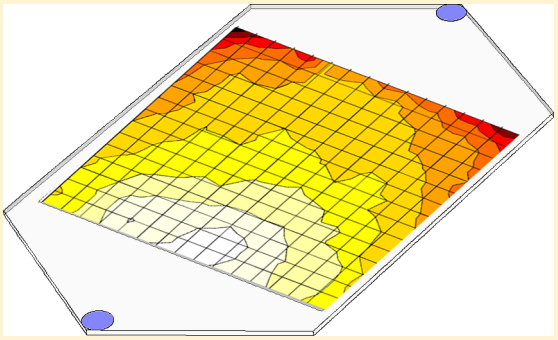

INTRODUCTION

There is an aspiration within the biosensor community to increase the functionality of biosensors through multiplexing recognition elements to enable simultaneous multianalyte detection. Within the defense industry this would facilitate monitoring of a range of threat materials while in the healthcare industry a single sample could be screened for a wide range of disease markers. The recent arrival of commercial array-based surface plasmon resonance (SPR) instruments has begun to address multiplexing requirements. Although these encompass significant developments for biosensor technology, a number of challenges are still to be addressed, particularly the choice of sensing surfaces employed. These must resist nonspecific binding of confounding material within potentially complex samples while specifically capturing targets of interest.

Traditionally, antibodies have provided the specificity required within biosensors to capture target material. Within SPR applications these have often been applied to a surface via a fluidics system. The advent of array-based SPR instrumentation has forced, at least temporarily, a move into the microarraying domain. Inkjet printing and microcontact printing have been applied to the fabrication of high density DNA arrays very successfully. Unfortunately the transfer of this knowledge to the protein arraying domain has proved more challenging than anticipated due to the more complex and varied nature of proteinaceous material.

Despite these challenges, reports have shown the successful use of array-based SPR instruments for a wide range of applications and with different classes of recognition elements. This has included the use of DNA-based recognition elements to study bacterial response regulators,[1] the study of protein binding kinetics with peptides as recognition elements,[2] the use of carbohydrates to specifically detect proteins,[3] and antibodies to specifically recognize low molecular weight[4] or cancer biomarkers.[5] Interested readers are directed to the review article by Scarano et al.[6] which considers a range of instrumentation, chip functionalities, technical approaches, and applications in more detail and that of Linman et al.[7] which considers the importance of the biosensor interface in achieving sensitive and selective responses.

The work reported here employed the BIAcore Flexchip, an array-based grating-coupled SPR (GC-SPR) instrument from GE Healthcare. This instrument monitors a 1 cm^2 active area, providing simultaneous analysis of up to 400 separate regions of interest (ROIs). A comprehensive description of the instrument and its functionality has been provided elsewhere.[8] Valuable characterization with proteinaceous analytes has been undertaken by the Sexton[9] and Myszka[8] groups. Their work has shown the Flexchip capable of undertaking kinetic analysis of Fab fragments capturing human tissue kallikrein 1 and the capture of IgG material by protein A/G. Both groups report no trend in kinetic constants with ligand location on the chip

Received: February 23, 2012
Revised: June 13, 2012
Published: August 10, 2012

surface and an overall variability of ca. 10%. This validation is particularly important for screening applications where bias introduced by ligand location on the surface could result in inappropriate down-selection.

Here we progress the understanding of large flow-cell array-based SPR instruments by considering the response observed upon binding of sporulated bacteria. Although not traditionally associated with the direct detection of microorganisms due to the size discrepancy between evanescent field (typically thought to extend 100−200 nm from the surface[10,11]) and microorganism diameter (e.g., *Bacillus anthracis* spores are ∼1 μm), SPR has successfully been used to directly detect living cells,[12] viruses,[13] and bacteria.[14−16] It is not possible to accurately determine kinetic information with microorganisms because of the range of molecular weights present. It is however possible to undertake, for example, quantitative screening of antibodies for their binding capacity at a range of concentrations with qualitative understanding of their kinetics.

We have used the Flexchip to investigate and understand the uniformity of response to particulate analytes across the flow cell. By considering the specific responses obtained for *Bacillus anthracis* spores and proteinaceous exosporium from *Bacillus anthracis*, binding to a single monoclonal antibody, we have resolved response contributions due to size effects. This has allowed confident screening of bacterial targets and optimal location of recognition elements in multianalyte applications, thus deepening the understanding of the complexities of multianalyte biodetection.

MATERIALS AND METHODS

Reagents. Gold Affinity Chips, BIAcore Flexchip Blocking Buffer 10x, human β-2 microglobulin (β-2 m), and monoclonal mouse antibody α-human β-2 microglobulin (α-β-2 m) were supplied by GE Healthcare (Buckinghamshire, UK). Phosphate-buffered saline (PBS, GIBCO PBS) was supplied by Invitrogen (Paisley, UK), and polyoxyethylenesorbitan monolaurate (Tween 20) and glycerol were obtained from Sigma-Aldrich Ltd. (Dorset, UK).

Rabbit polyclonal antibodies to *Bacillus atrophaeus* (α-BG) and ovalbumin (α-OA) were produced in-house. *Bacillus atrophaeus* (BG) was supplied by the Centre for Applied Microbiological Research (now the Health Protection Agency, Porton Down, UK). BG spores were heat-treated at 70 °C for 1 h and then cold shocked on ice for 30 min to remove any vegetative cells before washing 3 times via centrifugation at 9000 rpm for 10 min with resuspension of the pellet in distilled water.

A mouse monoclonal antibody to *Bacillus anthracis* (DSTL103) was developed in-house and produced by Detection Consumables Ltd. (Dorset, UK). *Bacillus anthracis* UM23Cl2 (UM23Cl2 spores), a double-cured derivative of the *Bacillus anthracis* Weybridge (Sterne) strain lacking both virulence plasmids (pX01 and pX02), and its exosporium isolate (UM23Cl2-exosporium) were prepared for use according to a literature procedure.[17] Pierce BCA Protein Assay (Fisher Scientific UK Ltd., Loughborough, UK) was used to quantify the amount of soluble proteinaceous material present within the UM23Cl2 spore preparation. This was calculated to be less than 0.4 μg mL^{-1} at the spore concentration used based on the observed limit of detection of the assay. All samples were stored at −20 °C until required.

Chip Preparation. Gold affinity chips were prepared by gentle sonication (frequency of 80 kHz and power of 80 W) in 70% v/v ethanol−water solution for 3 min followed by drying with a stream of nitrogen gas within the protective confines of a laminar flow hood. Chips were then transferred to the arraying chamber where the relative humidity was set to 70% at ambient temperature and pressure.

A piezoelectrically driven pipetting system, the Nano-Plotter NP1.2 (GeSiM mbH), was used to create discrete functional spots on the gold affinity chips. Before and after use a Nano-Tip micropipet (GeSiM mbH) was cleaned by at least three manual aspirations of a 70% v/v ethanol−water mixture in accordance with manufacturer's guidance. Immediately prior to use, the instrument-controlled washing protocol rinsed the tip with deionized water for 200 s. Optimization of the jetting parameters (piezo drive voltage and pulse width) was undertaken using the "Strobocheck" feature within the software. The software was used to define a 16 × 16 array of equally dispersed spots across the chip where antibodies would be deposited. Immediately before use, antibodies were diluted to a concentration of 200 μg mL^{-1} in PBS containing 30% glycerol v/v. For deposition, the tip was held 0.5 mm above the target surface and 3 drops (totaling ∼1.05 nL) deposited at each location creating antibody-containing spots of ca. 200 μm diameter. Between samples the tip was washed for a minimum of 20 s in deionized water using the instrument control software. Once antibody deposition was complete, the chip was placed in a sealed falcon tube and stored at 4 °C overnight.

For work with BG, two antibodies, α-BG (experimental) and α-OA (control), were deposited in two spatially separated blocks each comprising six spots. Control spots, containing no antibody were also deposited. For work with UM23Cl2 spores and UM23Cl2-exosporium, two antibodies, DSTL103 (experimental) and α-β-2 m (control), were deposited in an alternating fashion (Figure 1).

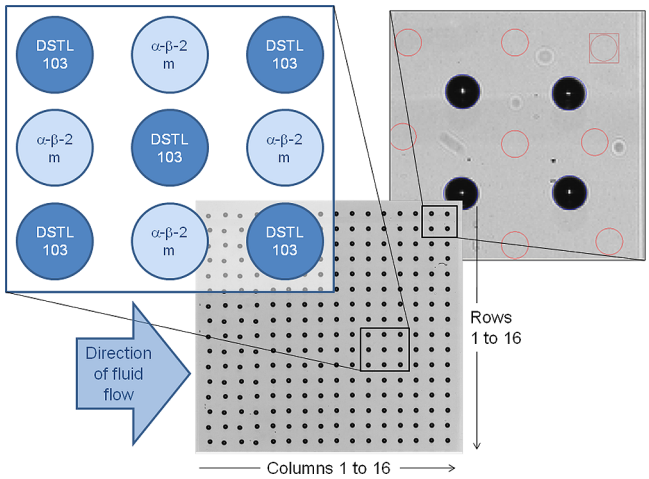

Figure 1. Schematic illustrating array format. Image of a 16 × 16 array of antibodies on a gold affinity chip (bottom center). Detail from this image (top right) after definition of ROIs (blue circles surrounding black antibody spots) and reference regions (red circles) illustrates their relative locations. A schematic (top left) illustrates the alternate composition of spots which contain the antibodies DSTL103 (dark blue circles) and α-β-2 m (light blue circles) and which extend across the array.

Chip Analysis. Arrayed chips were analyzed using a BIAcore Flexchip (GE Healthcare). The chip was prepared and docked in the instrument according to the manufacturer's instructions. The desired ligand ROIs (deposited antibody spots) and associated reference regions (arranged in the "checkerboard" fashion, Figure 1) were defined using the instrument control software. The surface was blocked with Flexchip Blocking buffer (diluted from stock to 1× in deionized water) using the control software blocking procedure (five cycles with 15 min pause) to reduce nonspecific binding between protein spots.

PBS containing 0.05% Tween 20 v/v (PBS(T)) was used throughout the experiments as running buffer and for sample dilution. A flow rate of 500 μL min^{-1} was employed. Surfaces were stabilized for 60 min before injection (with recirculation) of the sample followed by a 30 min dissociation period. Samples comprised β-2 m (3 μg mL^{-1}) for 30 min, UM23Cl2 spores (1×10^8 cfu mL^{-1}, washed three times to remove proteinaceous material) for 90 min and UM23Cl2-exosporium (10 μg mL^{-1}) for 90 min.

dx.doi.org/10.1021/la300782q | *Langmuir* 2012, 28, 12410−12416

Data was collected and reference corrected using the Flexchip Control and Evaluation software. Reference correction subtracts the average response of the four reference regions located around each ligand ROI from the ligand ROI response (Figure 1), thus removing contributions from nonspecific binding to the chip surface. The average response during a 60 s window commencing 100 s after the end of the sample injection was used to compare specific responses. For interchip comparisons, responses were normalized using the average specific response from each chip.

Modeling. Flow cell dimensions were determined through a combination of practical measurements and information supplied by GE Healthcare. The geometry is depicted in Figure 2. Buffer enters

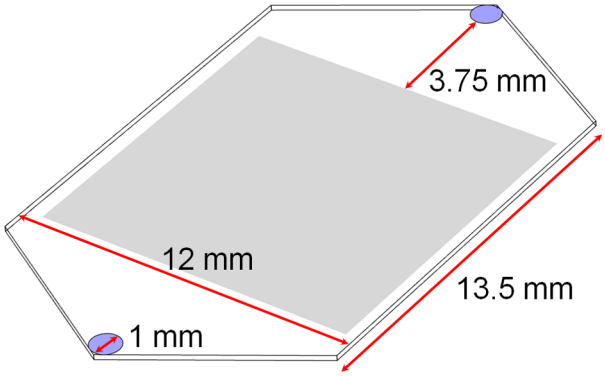

Figure 2. Schematic of the flow cell. Fluid inlet and outlet (blue circles) are located at the top of the flow cell while the SPR active region (gray square) lies at the bottom of the flow cell and is ~1 cm^2. The flow cell height is 180 μm when docked within the instrument.

and leaves the flow cell by circular openings in the top of the flow cell (blue circles in Figure 2). The SPR active area (a grating, gray square in Figure 2), lies centrally at the bottom of the flow cell.

Modeling was undertaken using the Fluent software, version 12.1 (ANSYS Inc., Canonsburg, PA). The Reynolds number, based on the height of the flow cell and the average velocity, was estimated to be less than 1; hence the steady-state flow was modeled as laminar. Double precision and second-order accuracy was used for the simulation. A constant velocity profile was defined on the flow cell inlet to obtain the desired flow rate of 500 μL min^{-1} with an outflow condition on the outlet to conserve mass. Convergence was achieved after 2000 iterations with all residuals being less than 10^{-10}. Approximately 3.3 million cells were used in this model.

RESULTS AND DISCUSSION

SPR Analysis: Spore Detection. To better understand the response from particulate analytes within array-based SPR instruments, antibodies were arrayed onto bare gold surfaces using the methods outlined above. This resulted in ROIs containing antibodies physisorbed on gold. Although it is widely accepted that the activity of antibodies can be adversely affected when immobilized onto surfaces, arising both from the method employed and their resultant proximity to a surface, many successful studies have been undertaken with both physisorbed and otherwise immobilized antibodies. We therefore chose physisorption as a means of immobilization within this study for its methodological simplicity, proven efficacy, and extensive use within the literature.

Initial testing sought to confirm the detection of whole spores by the Flexchip. For ease, an ACDP hazard group 1 material, BG, at 1×10^8 cfu mL^{-1}, was studied using an array of α-BG alongside the control antibody α-OA to confirm the specificity of the response. The average SPR responses from replicate spots of α-BG, α-OA, and spots containing only buffer (PBS) are presented in Figure 3 alongside a microscope image of an α-BG-functionalized spot postexposure. The microscope image reveals the presence of spores only for α-BG-functionalized areas. Low levels of nonspecific binding were visible between ROIs which was removed from the SPR response through reference correction (see methods). Control ROIs (functionalized with α-OA or simply PBS buffer) showed no binding of BG. The negative SPR response for these ROIs is a feature of the reference correction process and indicates that nonspecific binding to the reference regions is greater than binding to the control ROIs.

Spore detection is not traditionally associated with SPR technology due to the discrepancy between the penetration length of the evanescent field and the spore diameter. Various explanations exist for the ability of the Flexchip to detect spores. The most probable of these is the flow cell geometry and in particular the location of the sensing surface at its

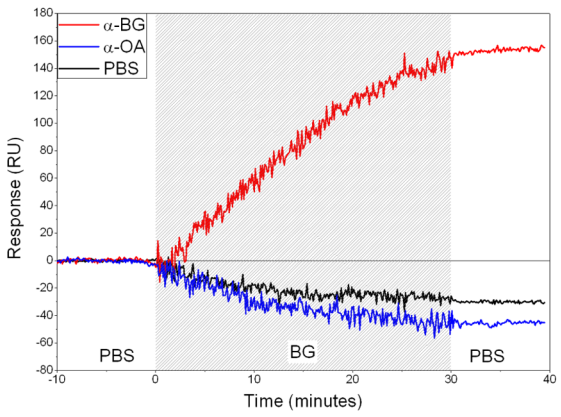

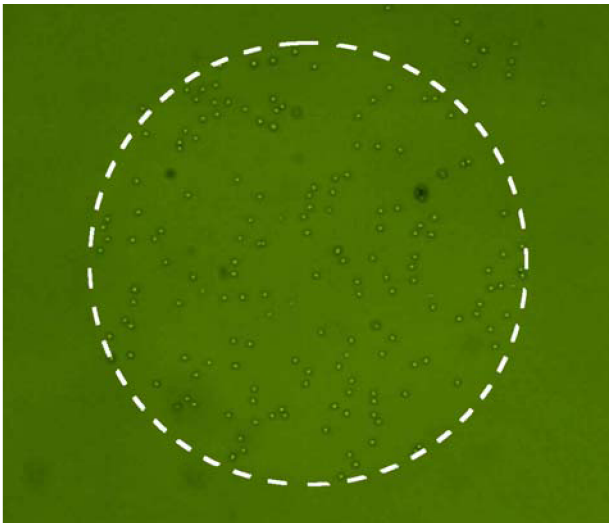

Figure 3. Sensorgram of the average response across the six replicate spots deposited (left) and a microscope image (right) for α-BG specifically binding BG. The dashed white line represents the boundary of the antibody-functionalized area of the microscope image. Low levels of nonspecific binding are visible.

dx.doi.org/10.1021/la300782q | *Langmuir* 2012, 28, 12410−12416

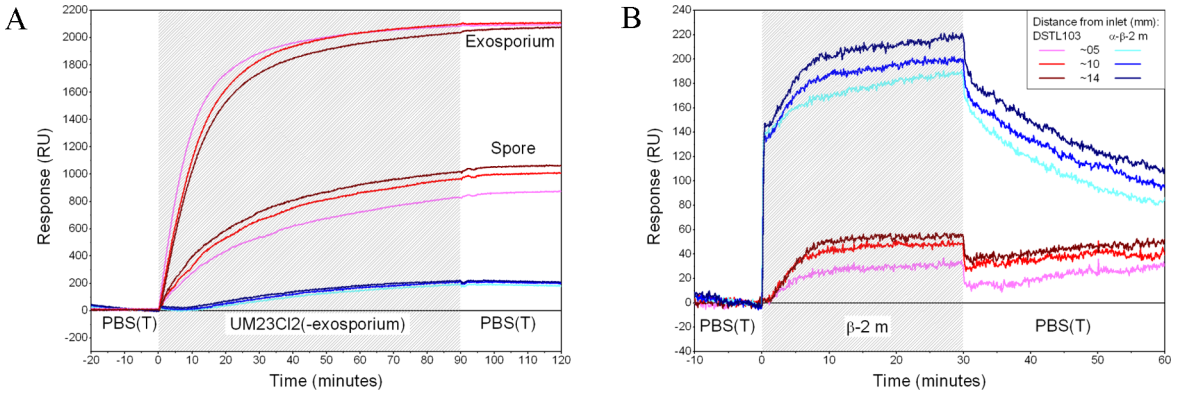

Figure 4. Typical sensorgrams for UM23Cl2 spores and UM23Cl2-exosporium (A), and microglobulin (B) binding to DSTL103 (red) and α-β-2 m (blue). Darker color shades indicate increased distance from the flow cell inlet while shaded areas depict the sample injection.

bottom. Thus, gravity can aid the movement of spores to the surface and facilitate their detection.

SPR Analysis: Impact of Analyte Size. To investigate size effects, two antibodies (α-β-2 m and DSTL103) were deposited onto the surface in an alternate fashion creating a 16 × 16 spot array uniformly covering the active area (Figure 1), sufficient to resolve any variations in response across the flow cell. The antibody α-β-2 m was chosen as a commercially available recognition element for which much published information is available,[18] providing confidence in the data. DSTL103 was chosen for the ability to specifically bind both UM23Cl2 spores (an analyte containing predominantly particulate material) and UM23Cl2-exosporium (an analyte containing only soluble material), allowing a single antibody to be used to probe the impact of analyte size without confounding contributions. By using antibodies to different targets, responses could be confirmed as specific.

Using the method described above, surfaces arrayed with DSTL103 and α-β-2 m were examined to establish specificity to their target analyte and the absence of cross reactivity. Representative sensorgrams taken from points located across the length of the flow cell are presented in Figure 4. As well as confirming specificity, these data highlighted significant differences in the affinity of the two antibodies. DSTL103 was found to have a high affinity to both UM23Cl2 spores and UM23Cl2-exosporium (Figure 4a), with little dissociation observed upon a return to running buffer after the sample injection. In contrast, α-β-2 m was found to have a much lower affinity to its target antigen, β-2 m (Figure 4b), showing significant dissociation with time.

Nonspecific response levels between the antibodies were considered acceptable. The average response from α-β-2 m to β-2 m was (160 ± 20) RU with a nonspecific response from DSTL103 of (33 ± 8) RU (equal to 20% of the average specific response). The low response by α-β-2 m to β-2 m in comparison to the response seen by DSTL103 to UM23Cl2-exosporium is probably a consequence of their relative molecular weights. β-2 m (11.5 kDa) is significantly smaller than the UM23Cl2-exosporium which comprises a variety of proteins whose molecular weights extend up to 98 kDa,[17] resulting in larger responses from similar numbers of binding events. The coefficient of variation for specific β-2 m responses across multiple chips was found to be ~11%, similar to the variability in kinetic constants reported by others.[8,9]

The average response for DSTL103 to UM23Cl2 spores across three replicate chips was (1100 ± 200) RU, with α-β-2 m nonspecific response of (280 ± 20) RU (or 29% of the average specific response). Chip-to-chip variation was an important contributor to the uncertainty with noticeable variation in response magnitude for chips produced in an identical fashion. Within a single chip the coefficient of variation was typically around 9%, while between chips it was 16%. For UM23Cl2-exosporium, the average response by DSTL103 was significantly greater than for spores at (2100 ± 50) RU. This most likely reflects the increased binding density possible within the evanescent field due to the smaller size of exosporium proteins compared to the intact spore. Although the UM23Cl2 spore binding had not reached equilibrium, the trend is for sensorgrams to continue in a parallel fashion rather than converge. This has been confirmed with longer injection times where binding was taken to equilibrium (data not shown).

Previous studies which have modeled the concentration profile within a flow cell for soluble materials have indicated that sample depletion may occur through the course of the flow cell, resulting in lower levels of binding as distance from the inlet increases.[8] To investigate whether analyte size influenced the response profile across the flow cell, we determined the response as a function of spot location for both proteinaceous and particulate antigens. Binding responses from three replicate chips were combined. First, data points on each chip corresponding to the location of control antibodies were estimated using the average of surrounding responses. Responses were then normalized as described above, and an average across replicate chips was determined. Using the same approach for both UM23Cl2 spores and UM23Cl2-exosporium data, a single normalized response at discrete locations across the array was determined (Figure 5).

The results with UM23Cl2 spores (Figure 5a), a predominantly particulate antigen containing less than 0.4 μg mL^{-1} of soluble material as determined from BCA Protein Assay, show a lower than average response closest to the inlet, increased response on the edges parallel to the direction of flow, and the highest response in the corners furthest from the flow cell inlet. This trend was apparent across four independently prepared chips regardless of chip orientation during the arraying process. Additionally, a chip produced via contact arraying showed the same trend (data not shown). The responses for the soluble antigen, UM23Cl2-exosporium binding to the same antibodies, Figure 5b, are more uniform across the active area of the chip. Similarly, β-2 m binding to α-β-2 m antibodies produced a relatively uniform response across

dx.doi.org/10.1021/la300782q | Langmuir 2012, 28, 12410−12416

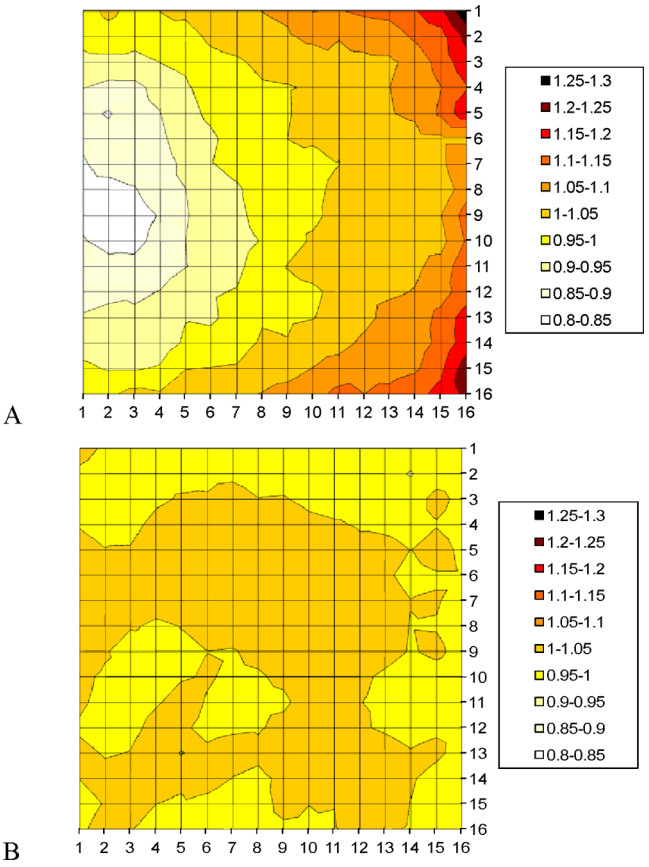

Figure 5. Normalized responses for DSTL103 to a particulate analyte, UM23Cl2 spores (a), and a soluble analyte, UM23Cl2-exosporium (b). Sample flow is from left to right. Data is presented on identical scales for comparative purposes.

the surface. Consequently, it is proposed that the pattern observed with UM23Cl2 spores results from the combination of flow cell geometry (which determines the fluid flow), the particulate nature of the analyte, and the size of the particles. When coupled with the data presented in Figure 3, this confirms that label-free whole spore detection through SPR is achievable, despite the size discrepancy between analyte and evanescent field, in agreement with previous reports.[14−16]

Flow Cell Modeling. To better understand the origins of the responses observed with particulate analytes, we undertook preliminary computational fluid dynamics modeling of the flow cell as described above. Previous modeling of analyte solutions and surface gradients by Rich et al.[8] for proteinaceous materials suggests that the highest analyte concentration, and consequently the highest response, is observed close to the inlet, producing an inverse response pattern compared to that observed here with spores. A more recent publication has highlighted that in contrast to soluble material, the detection of microorganisms by sensing surfaces is driven by hydrodynamics and sedimentation forces, making the optimal flow conditions very different to those best suited to the detection of soluble analytes.[19] This is supported by two further publications by the Sjollema group who report that sedimentation dominates mass-transport within parallel plate flow cells, akin to that used within the Flexchip.[20,21]

Calculations have revealed that the Flexchip flow cell geometry is conducive to laminar flow, and the stream lines show an absence of eddies and recirculation. The simplicity of the flow belies the complexities of the interactions present in the system. Analytes will experience not only hydrodynamic and sedimentation effects but also the attractive force of antibodies once they are in close proximity to the sensing surface. Antibodies are able to both capture and release their target analytes, dependent on affinity, ionic strength, pH, and the shear forces they are exposed to.

The impact of diffusion and gravity on particulate trajectories within the flow cell should also be considered. Applying Einstein's equation for the diffusion coefficient of a substance in terms of particulate radii, $D = (k_B T)/(3\pi\mu d)$, where k_B is the Boltzmann constant, T the absolute temperature (298 K), μ the viscosity ($\sim 10^{-3}$ Pa s), and d the particle diameter ($\sim 1.1 \times 10^{-6}$ m), we find an approximate value for the diffusion coefficient of *Bacillus anthracis* spores in buffer of 4×10^{-13} m^2 s^{-1}. Using this value, an upper limit on the diffusional mass transfer coefficient in a parallel sided laminar flow situation can be estimated according to the equation[22]

$$k_d = \frac{D}{H} \times \frac{\left[\frac{VH^2}{3Dx}\right]^{1/3}}{0.893}$$

where H is the height of the flow cell (180 μm), x is distance from the inlet, chosen to be approximately half way along the flow cell ($\sim$0.01 m), the velocity $V = Q/(WH)$ where Q is the flow rate (taken as 500 μL min^{-1}) and W the flow cell width (0.012 m). Using these values, k_d for *Bacillus anthracis* spores in buffer is estimated to be approximately 6×10^{-8} m s^{-1}.

Similarly, a gravitational mass transfer coefficient or settling velocity, k_g can be estimated via the equation:

$$k_g = \frac{gd^2}{18\mu}(\rho_s - \rho)$$

where ρ_s and ρ are the density of the buffer solution (1162 kg m^{-3}) and spore (1002 kg m^{-3}), respectively, giving rise to an estimate for k_g of 9×10^{-8} m s^{-1}. It is apparent that estimates of the diffusive and gravitational transfer coefficients acting on spores are of the same order of magnitude, implying that both effects should be included within any model. It is important to note that the upper limit of diffusional flux does not account for a finite rate of particle binding to an antibody-functionalized surface nor drag forces acting on the particle. An accurate model will require representation of both the particle−surface interactions and drag.

Preliminary exploration of the flow cell fluid dynamics has given rise to the hypothesis that the response observed with particulate antigen predominantly arises from a combination of diffusion, shear, and gravitational effects. The wall shear stress reveals a symmetrical dependence both parallel and perpendicular to the direction of flow (Figure 6) that in part reflects the response trend presented in Figure 5. Regions of high shear stress associated with the inlet and outlet of the flow cell are attributable to the increased velocity component parallel to the surface of the flow cell as it narrows upon approach to these regions. Consequently, we propose that the low response observed for particulate antigens toward the inlet of the flow cell may result from the higher shear stress in this region either preventing capture or removing weakly bound material from the surface. It is noteworthy that shear forces believed to be in the region of tens of picoNewtons can remove bacterial spores from chemically functionalized surfaces.[23] Data for the disruption of antibody−antigen complexes are only available

dx.doi.org/10.1021/la300782q | *Langmuir* 2012, 28, 12410−12416

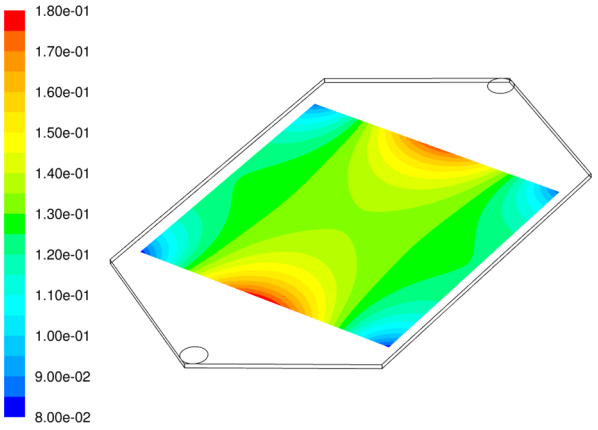

Figure 6. Predicted wall shear stress (Pa) contours across the active sensing region of the flow cell. High stress (red) is apparent toward the inlet (lower left circle) and outlet (upper right circle) with lower stress (blue) toward edges and corners of the active area.

perpendicular to the surface and indicate that forces of 50−100 pN are required.[24] The directionality of this force makes the impact of shear stress here challenging to interpret. If residual free exosporium protein or other soluble material were present in the spore preparation, two possibilities exist. A uniform contribution across the whole flow cell may be included in the spore response, in agreement with the data presented for the soluble analyte (Figure 5b). Alternatively, were sufficient binding of soluble material to occur such as to cause sample depletion, it might be expected that the response would decrease through the flow cell, in agreement with the models presented by Rich et al..[8] Measurements by BCA Protein Assay however suggest that minimal amounts of soluble material from the UM23Cl2 spore preparation are present and thus the spatial dependency of the response can confidently be attributed to the particulate nature of the analyte.

Previous unreported work by ourselves coupled with the report by Langer et al.[19] suggests that for particulate antigens, gravity can significantly aid detection. It is therefore proposed that as particulate analytes progress through the flow cell, they begin the process of sedimentation, bringing greater numbers progressively closer to the surface. Consequently, a higher response is seen toward the outlet, as particles have been in the flow cell for a longer period of time and thus gravity has brought them closer to the surface, facilitating binding.

The higher responses at the edges of the flow cell in comparison to those in the middle could be a consequence of both gravitational and hydrodynamic effects. Particles in this outer region are moving more slowly than their centrally positioned counterparts and have therefore been in the flow cell longer; hence, gravity will have brought a greater number into close proximity with the surface. The lower shear stress in this region may also serve to aid capture. The maximal response seen at the two corners of the active region closest to the outlet is a culmination of these factors.

Our hypothesis is supported by the recent work of the Sjollema group[20,21] who proposed that the much used Smoluchowski−Levich approximation of the two-dimensional convective-diffusive equation may not adequately describe the movement of bacteria within a parallel plate flow chamber but that sedimentation dominates mass-transport. Consequently, the response observed is a function of both flow rates and distance from the flow cell inlet.

In light of our findings, we propose the use of a correction factor when undertaking work with particulate antigens within the Flexchip and other instruments possessing similar flow dynamics. This will enable the exploitation of the instrument for applications such as ligand screening with particulate antigens as well as the proteinaceous materials for which it was originally intended. Without some form of correction, unfair bias toward ligands in preferential binding regions will occur. It is likely that binding responses are strongly influenced by flow rate and flow cell geometry, thus for *Bacillus anthracis* spores (of ca. 1 μm diameter) within the Flexchip, with a flow rate of 500 μL min^{-1}, the responses presented in Figure 5a may be used as a correction factor. As expected, application of this correction factor to data from a single chip results in a significant reduction in variability, from ca. 9% to 3%.

■ CONCLUSIONS

The simultaneous, high confidence, and sensitive detection of a wide variety of microorganisms is a challenge within the biosensing arena. Multiplexing of recognition elements, such as antibodies, may go some way to providing this capability; however, it is important to understand the impact of analyte size on the sensor response obtained. A GC-SPR instrument, the Flexchip, was used to compare the uniformity of response from specific binding of particulate (*Bacillus anthracis* spores) and soluble (exosporium from *Bacillus anthracis*) antigens to a monoclonal antibody. This highlighted a spatial dependency on response for particulate samples which, through preliminary modeling, we suggest arises from a combination of shear and gravitational forces. This result has important implications for both screening and pathogen detection applications. We propose that for screening applications employing particulate antigen, correction factors should be employed to correct the bias introduced by the flow cell. For applications considering the simultaneous monitoring of multiple microorganisms with a range of sizes, the location of recognition elements may be optimized to provide optimal sensitivity through preferential binding.

■ AUTHOR INFORMATION

Corresponding Author

*E-mail: necant@dstl.gov.uk.

Notes

The authors declare no competing financial interest.

■ ACKNOWLEDGMENTS

We acknowledge the UK Ministry of Defence for funding, and thank GE Healthcare, particularly Henrik Berling, for kindly supplying microglobulin antigen and antibodies, and for invaluable discussions pertaining to the Flexchip instrument. Published with permission of the Defence Science and Technology Laboratory on behalf on the Controller of HMSO.

■ REFERENCES

(1) Smith, E. A.; Erickson, M. G.; Ulijasz, A. T.; Weisblum, B.; Corn, R. M. Surface Plasmon Resonance Imaging of Transcription Factor Proteins: Interactions of Bacterial Response Regulators with DNA Arrays on Gold Films. *Langmuir* **2003**, *19*, 1486−1492.

(2) Wegner, G. J.; Wark, A. W.; Lee, H. J.; Codner, E.; Saeki, T.; Fang, S. P.; Corn, R. M. Real-time Surface Plasmon Resonance Imaging Measurements for the Multiplexed Determination of Protein Adsorption/Desorption Kinetics and Surface Enzymatic Reactions on Peptide Microarrays. *Anal. Chem.* **2004**, *76*, 5677−5684.

(3) Karamanska, R.; Clarke, J.; Blixt, O.; Macrae, J. I.; Zhang, J. Q. Q.; Crocker, P. R.; Laurent, N.; Wright, A.; Flitsch, S. L.; Russell, D. A.; Field, R. A. Surface Plasmon Resonance Imaging for Real-Time, Label-Free Analysis of Protein Interactions with Carbohydrate Microarrays. *Glycoconjugate J.* **2008**, *25*, 69−74.
(4) Ladd, J.; Taylor, A. D.; Piliarik, M.; Homola, J.; Jiang, S. Y. Label-Free Detection of Cancer Biomarker Candidates using Surface Plasmon Resonance Imaging. *Anal. Bioanal. Chem.* **2009**, *393*, 1157−1163.
(5) Lee, H. J.; Nedelkov, D.; Corn, R. M. Surface Plasmon Resonance Imaging Measurements of Antibody Arrays for the Multiplexed Detection of Low Molecular Weight Protein Biomarkers. *Anal. Chem.* **2006**, *78*, 6504−6510.
(6) Scarano, S.; Mascini, M.; Turner, A. P. F.; Minunni, M. Surface Plasmon Resonance Imaging for Affinity-Based Biosensors. *Biosens. Bioelectron.* **2010**, *25*, 957−966.
(7) Linman, M. J.; Abbas, A.; Cheng, Q. A. Interface Design and Multiplexed Analysis with Surface Plasmon Resonance (SPR) Spectroscopy and SPR Imaging. *Analyst* **2010**, *135*, 2759−2767.
(8) Rich, R. L.; Cannon, M. J.; Jenkins, J.; Pandian, P.; Sundaram, S.; Magyar, R.; Brockman, J.; Lambert, J.; Myszka, D. G. Extracting Kinetic Rate Constants from Surface Plasmon Resonance Array Systems. *Anal. Biochem.* **2008**, *373*, 112−120.
(9) Wassaf, D.; Kuang, G.; Kopacz, K.; Wu, Q.-L.; Nguyen, Q.; Toews, M.; Cosic, J.; Jaques, J.; Wiltshire, S.; Lambert, J.; Pazmany, C. C.; Hogan, S.; Ladner, R. C.; Nixon, A. E.; Sexton, D. J. High-Throughput Affinity Ranking of Antibodies using Surface Plasmon Resonance Microarrays. *Anal. Biochem.* **2006**, *351*, 241−253.
(10) Snopok, B. A.; Goltsov, Y. G.; Kostyukevich, E. V.; Matkovskaja, L. A.; Shirshov, Y. M.; Venger, E. F. Self-Assembled Multilayer Superstructures as Immobilization Support for Bioreceptors. *Sens. Actuators, B* **2003**, *95*, 336−343.
(11) Wofsy, C.; Goldstein, B. Effective Rate Models for Receptors Distributed in a Layer Above a Surface: Application to Cells and Biacore. *Biophys. J.* **2002**, *82*, 1743−1755.
(12) Yanase, Y.; Hiragun, T.; Kaneko, S.; Gould, H. J.; Greaves, M. W.; Hide, M. Detection of Refractive Index Changes in Individual Living Cells by means of Surface Plasmon Resonance Imaging. *Biosens. Bioelectron.* **2010**, *26*, 674−681.
(13) Park, T. J.; Lee, S. J.; Kim, D. K.; Heo, N. S.; Park, J. Y.; Lee, S. Y. Development of Label-free Optical Diagnosis for Sensitive Detection of Influenza Virus with Genetically Engineered Fusion Protein. *Talanta* **2012**, *89*, 246−252.
(14) Bergwerff, A. A.; van Knapen, F. Surface Plasmon Resonance Biosensors for Detection of Pathogenic Microorganisms: Strategies to Secure Food and Environmental Safety. *J. AOAC Int.* **2006**, *89*, 826−831.
(15) Leonard, P.; Hearty, S.; Quinn, J.; O'Kennedy, R. A Generic Approach for the Detection of Whole *Listeria monocytogenes* Cells in Contaminated Samples using Surface Plasmon Resonance. *Biosens. Bioelectron.* **2004**, *19*, 1331−1335.
(16) Skottrup, P. D.; Nicolaisen, M.; Justesen, A. F. Towards On-Site Pathogen Detection using Antibody-Based Sensors. *Biosens. Bioelectron.* **2008**, *24*, 339−348.
(17) Redmond, C.; Baillie, L. W. J.; Hibbs, S.; Moir, A. J. G.; Moir, A. Identification of Proteins in the Exosporium of *Bacillus anthracis*. *Microbiology* **2004**, *150*, 355−363.
(18) Lofas, S.; Johnsson, B.; Tegendal, K.; Ronnberg, I. Dextran Modified Gold Surfaces for Surface Plasmon Resonance Sensors: Immunoreactivity of Immobilized Antibodies and Antibody-Surface Interaction Studies. *Colloids Surf., B.* **1993**, *1*, 83−89.
(19) Langer, V.; Niessner, R.; Seidel, M. Stopped-Flow Microarray Immunoassay for Detection of Viable *E. coli* by use of Chemiluminescence Flow-Through Microarrays. *Anal. Bioanal. Chem.* **2011**, *399*, 1041−1050.
(20) Li, J.; Busscher, H. J.; Norde, W.; Sjollema, J. Analysis of the Contribution of Sedimentation to Bacterial Mass Transport in a Parallel Plate Flow Chamber. *Colloids Surf., B* **2011**, *84*, 76−81.
(21) Li, J.; Busscher, H. J.; van der Mei, H. C.; Norde, W.; Krom, B. P.; Sjollema, J. Analysis of the Contribution of Sedimentation to Bacterial Mass Transport in a Parallel Plate Flow Chamber Part II: Use of Fluorescence Imaging. *Colloids Surf., B* **2011**, *87*, 427−432.
(22) Middleman, S. *An Introduction to Mass and Heat Transfer: Principles of Analysis and Design*; John Wiley & Sons, Inc.: New York, 1998.
(23) Bowen, W. R.; Fenton, A. S.; Lovitt, R. W.; Wright, C. J. The Measurement of *Bacillus mycoides* Spore Adhesion using Atomic Force Microscopy, Simple Counting Methods, and a Spinning Disk Technique. *Biotechnol. Bioeng.* **2002**, *79*, 170−179.
(24) Verbelen, C.; Gruber, H. J.; Dufrene, Y. F. The NTA-His6 Bond is Strong Enough for AFM Single-Molecular Recognition Studies. *J. Mol. Recognit.* **2007**, *20*, 490−494.